

Rheological aging and rejuvenation in solid friction contacts

L. Bureau, T. Baumberger and C. Caroli

Groupe de Physique des Solides (UMR 7588), Universit es Paris 6 & 7, 2 place Jussieu, 75251 Paris Cedex 05, France.

Abstract. We study the low-velocity ($0.1\text{--}100 \mu\text{m}\cdot\text{s}^{-1}$) frictional properties of interfaces between a rough glassy polymers and smooth silanized glass, a configuration which gives direct access to the rheology of the adhesive joints in which shear localizes. We show that these joints exhibit the full phenomenology expected for confined quasi 2D soft glasses: they strengthen logarithmically when aging at rest, and weaken (rejuvenate) when sliding. Rejuvenation is found to saturate at large velocities. Moreover, aging at rest is shown to be strongly accelerated when waiting under finite stress below the static threshold.

PACS.

1 Introduction

Surfaces of macroscopic solids in general present some degree of roughness on the small — typically micrometric — scale. For this reason, most extended interfaces between two nominally flat solids are of the multicontact type, i.e. composed of a sparse set of real contacts between load-bearing asperities (Fig.1). Their typical size lies in the $1\text{--}10 \mu\text{m}$ range, and they bear average normal stresses \bar{p} of the order of the yield stress Y of the weaker bulk material [1].

In frictional sliding, it is in the nanometer-thick region — the “joint” — where the two surfaces come into molecular contact and feel the short-range adhesive interactions, that shear localizes, which indicates that the joint is mechanically weaker than the cohesive bulk [2].

Following Tabor [1], the solid friction force F needed to slide one solid against the other at relative velocity \dot{x} reads:

$$F = \sigma_s \Sigma_r \quad (1)$$

with Σ_r the total real area of contact, and σ_s the shear stress within microcontacts.

It is now well established that, at low velocities, the variations of the friction force are governed by the competition between two effects:

(i) *Geometric* aging: since $\bar{p} \sim Y$, the load-bearing asperities creep plastically, hence Σ_r increases quasi-logarithmically with contact duration Φ , which may thus be termed “geometric age”. When the interface is at rest, $\Phi = t$. When motion starts, contacts get gradually destroyed, after a lifetime or age Φ , and replaced by fresh ones. So, while the interface sits still, it ages (strengthens), when it slides, it rejuvenates (weakens). This is reflected in the so-called static friction peak observed when setting the system into motion by loading it at constant velocity [3].

(ii) Velocity dependence of the sliding stress σ_s : For various types of such rough/rough multicontact interfaces

(polymer glasses [2], rocks [4,5], paper [6]) the analysis of the sliding dynamics has led to conclude that, for \dot{x} typically in the $1\text{--}100 \mu\text{m}\cdot\text{s}^{-1}$ range, and up to experimental accuracy:

$$\sigma_s(\dot{x}) \cong \sigma_{s0} \left(1 + \alpha \ln \frac{\dot{x}}{V_0} \right) \quad (2)$$

with V_0 some reference velocity in this range. For most systems α lies in the 10^{-2} range. This rheology can be interpreted as resulting from thermally activated “depinning” dissipative events occurring within the adhesive joint and involving activation volumes in the $(\text{nm})^3$ range [2,7].

This is consistent with the following qualitative description of adhesive solid friction joints:

(i) A joint is a molecularly disordered, quasi-2D medium with thickness h of nanometric order. This is obviously the case when the bulk solids themselves are amorphous. It should also be so for a vast majority of solids ordered in the bulk, due to nanometric surface roughnesses, defects in the bulk, atomic misorientation between surfaces, and the frequent presence of adsorbates [8].

(ii) At rest under zero shear stress, this highly confined medium is a solid. Indeed it is found to respond elastically to a small amplitude shear force.

(iii) When this force reaches the static friction threshold, $F_s = \mu_s W$ (with W the normal load and μ_s the static friction coefficient), sliding sets in.

Such a phenomenology entails that frictional sliding can be understood as plastic flow of this 2D confined medium sheared at a deformation rate \dot{x}/h proportional to the interfacial sliding velocity. The static threshold then corresponds to what is usually called, in the language of bulk plasticity, the yield stress.

Recent theoretical [9,10,11,12] and experimental [13, 14,15] developments in the rheology of complex fluids and (e.g. soft) glasses, have brought to light the important

fact that the main characteristics of such rheologies can be interpreted as resulting from the interplay between:

(i) Glass-like aging: As a quenched amorphous structure relaxes down its glassy energy landscape, the system becomes mechanically stronger. This age-strengthening is usually roughly logarithmic.

(ii) Rejuvenation by motion: In the plastic regime, dissipative events, instead of being solely due to activation by (thermal or dynamical) noise, are accelerated by the stress-induced biasing of the energy landscape. The “young”, shallow energy states which were depopulated as aging pushed the system into “older”, deeper ones, thus get repopulated: The sheared soft glass rejuvenates.

If the characterization of solid friction proposed above is truly relevant, it should therefore be possible to evidence *structural* aging *vs* rejuvenation effects in the rheology of adhesive joints. If such effects are present, a more direct — hence accurate — experimental study of the fine variations of the frictional stress should reveal that σ_s not only depends on the instantaneous deformation rate \dot{x}/h , but also on the previous history of the joint.

In this article we show, on the basis of a detailed experimental study of the frictional dynamics of a {rough PMMA/float glass} interface, that such is indeed the case. The use of such a configuration, in which the microcontacts permanently retain their identity, enables us to get rid of the *geometric* aging/rejuvenation effects which are predominant for rough/rough interfaces. We are thus able to show that, while an adhesive joint strengthens quasi-logarithmically as it ages at rest, it rejuvenates when sliding. Moreover, we report experiments in which the joint ages under a finite shear stress below the static threshold. They clearly demonstrate that, the larger this applied stress, the faster the aging dynamics of the joint. All this phenomenology proves that a frictional joint can be considered as a confined *2D* soft glass.

In section 2 we describe the system and measurement setup, and the experimental procedures. Section 3 reports the experimental results, which are discussed in section 4.

2 Experimental setup and system preparation

2.1 Sample preparation

The system consists of a slider and a track. The slider is a poly(methyl methacrylate) [PMMA] block, with thickness 10 mm and a nominal area $20 \times 70 \text{ mm}^2$, sliding along its longer dimension. The sliding surface is roughened by hand-lapping against a flat reference glass plate with SiC powder (GRIT 400). The resulting r.m.s. roughness is $1.3 \mu\text{m}$. After lapping, the surface is thoroughly rinsed with distilled water and dried by an Ar flux.

The track is a float soda lime glass $120 \times 120 \text{ mm}^2$ plate, of thickness 10 mm, with subnanometric roughness on the micrometer scale. Its surfaces are prepared as follows :

(i) Cleaning

The plate, degreased with methanol, ethanol and acetone, is sonicated first in a 2% solution of RBS detergent for 15 minutes at 50°C , then in ultrapure milli-Q water.

After drying it by a N_2 flux, ultimate cleaning is performed in a UV-ozone reactor for 2 hours under the steady O_2 flux 0.5 l/min, both surfaces being successively exposed to the UV light.

We thus obtain what we will call “bare” glass. In the cases where we use it as such, the plate is immediately transferred from the clean room into the glove box in which all experiments are performed.

(ii) Silanization

Most track samples are silanized before use, with the short molecule (1,1,1,3,3,3) hexamethyl disilazane, in a vacuum chamber. Prior to silanization, the plate is exposed for 12 hours to a saturated water vapor in order to maximize the number of reactive Si-OH surface sites. After pumping out this vapor, the evacuated chamber and the flask containing 1 ml of silane are separately heated up to 90°C , then put in communication, which results in total silane evaporation. The reaction is carried on at 90°C for either 1 (D1 tracks) or 5 days (D5 tracks).

After cooling, the samples are transferred to the glove box, where we maintain a small Ar overpressure, in the presence of a desiccant resulting in 8–10% relative humidity. All experiments are performed at temperature 20°C , well below the PMMA glass transition temperature ($T_g \simeq 110^\circ\text{C}$).

2.2 Measurement setup

The mechanical setup has been described in detail elsewhere [3]. It is schematized on Figure 1. The normal load on the interface is provided by the slider dead weight, $W = 7.7 \text{ N}$. The slider is driven by a stepping motor through a loading spring of stiffness $K = 8 \times 10^{-2} \text{ N}/\mu\text{m}$, the elongation of which, measured with the help of a capacitive sensor, yields the tangential force to within 10^{-4} N . Driving velocities range between 10^{-1} and $10^2 \mu\text{m/s}$.

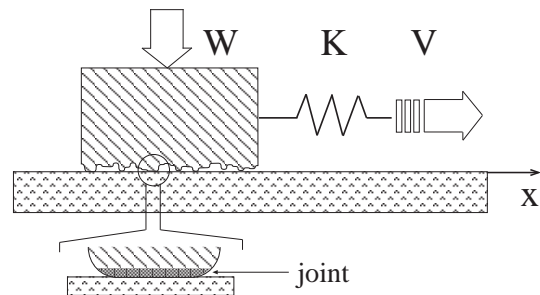


Fig. 1. Experimental setup: the PMMA sliding block, of weight W , is loaded through a spring of stiffness K driven at velocity V , along the glass track. Blow-up: microcontact between a PMMA asperity and the track.

2.3 Preparing an interface of constant Σ_r

In a preliminary series of experiments, the slider and track are brought into contact at an initial instant $t = 0$. We

then measure the dynamic friction coefficient $\mu_d = F/W$ in stationary sliding at $V_0 = 10 \mu\text{m/s}$, at successive times t_i ranging from ~ 10 to $\sim 10^5$ seconds. In between two measurements, the driving is stopped. After such a stop, the slider slows down, and ultimately stops (after a few seconds; see Figure 3) at a finite force level F_{stop} where no creep motion is detectable any longer. As shown on Figure 2, $\mu_d(V_0)$ is found to increase quasi-logarithmically with the time t elapsed from the moment of first contact. We have checked that $\mu_d(V_0 | t)$ is independent of the number and distribution of the t_i 's.

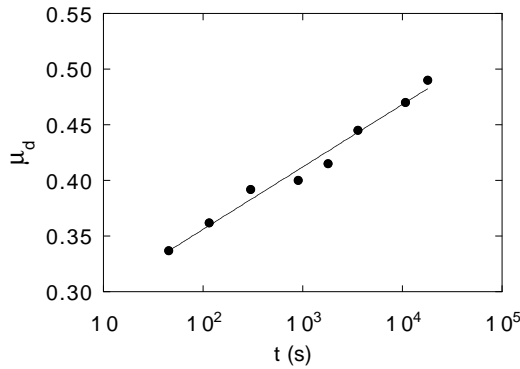


Fig. 2. Evolution, on a bare glass track, of the dynamic friction coefficient μ_d at velocity $V_0 = 50 \mu\text{m.s}^{-1}$ with time t elapsed from the creation of the interface. Line: best logarithmic fit.

This result can be attributed to the geometric aging of a population of contacts *which retain their identity during sliding*, in agreement with observations from optical imaging [16] of the sliding interface [17]. Indeed, in this case, the geometric age of the microcontacts simply reads $\Phi = t$, and :

$$\Sigma_r(t) = \Sigma_0 \left[1 + m \ln \left(1 + \frac{t}{\tau} \right) \right] \quad (3)$$

For PMMA at room temperature, τ has been estimated [3] to be at most of order 10^{-2} s, and $m \approx 10^{-2}$.

The measured logarithmic slope, $d\mu_d(V_0 | t)/d(\ln t) = 2.3 \cdot 10^{-2}$, yields a time evolution of Σ_r compatible with that deduced from the increase with waiting time of the static friction coefficient of a {rough/rough} PMMA interface: $d\mu_s/d(\ln t) = 1.7 \cdot 10^{-2} \pm 4 \cdot 10^{-3}$.

The situation encountered here is to be contrasted with the rough/rough configuration, in which sliding permanently destroys the microcontacts and replaces them by fresh ones. The use of a rough/flat system enables us to take advantage of the quasi-saturation associated with logarithmic growth, by performing experimental runs of limited duration Δt on an interface of geometric age $\Phi \gg \Delta t$. Typically, for all the results presented below, Φ ranges from $\sim 10^4$ to $\sim 10^5$ s, while $\Delta t < 1$ hour. Σ_r variations are then negligible, giving us access to the fine variations of the ‘‘rheological stress’’ σ_s .

3 Experimental results

3.1 Friction force level versus silanization

A first, rough characterization of the effect of the physico-chemical state of the glass surface is provided by the value $\bar{\mu}$ of μ_d measured at some fixed V_0 . Indeed, the friction force variations to be described below, which provide insight into the frictional joint dynamics, are always quite small as compared with the average level.

First of all, as can be expected for such a highly wettable surface, bare glass tracks yield highly scattered $\bar{\mu}$ -levels, ranging between 0.4 and 0.7

Silanization results in a sizeable decrease of both the average friction level and its scatter. Namely, for D1 tracks, $\bar{\mu}$ lies between 0.25 and 0.36. For more thoroughly silanized, D5 samples, $\bar{\mu}$ ranges from 0.13 to 0.2 – a very low level for unlubricated friction [1].

It is worth mentioning that contact angle measurements performed with pure water drops hardly permit to distinguish between D1 and D5 surfaces. The contact angle for both types of tracks is $85^\circ \pm 5^\circ$, compatible with previous measurements for short chain silanes [18]. This points towards the high sensitivity of solid friction as a probe of small scale chemical inhomogeneity of extended surfaces.

In view of the poor reproducibility of the results on nominally bare surfaces, clearly resulting from the presence of uncontrolled adsorbates, most of the results reported below have been obtained with D1 and D5 silanized glass tracks.

3.2 Static friction peak as a proof of structural aging

We prepare an ‘‘old’’ interface, with geometric age t_0 , on which we then perform a set of ‘‘stop-and-go’’ experiments. That is, starting from steady sliding at velocity V_0 , the drive is stopped, and the slider left at rest under its self-selected tangential force F_{stop} (see 3). After waiting a time t_w after the drive has been stopped, loading is resumed at the same V_0 . The corresponding force record, shown on Figure 3, exhibits a so-called static friction peak. Namely :

(i) In a first regime, F increases linearly, at the rate KV_0 corresponding to the elastic loading of the non sliding system. The interface is pinned.

(ii) This static regime ends at the peak value $F_s = \mu_s W$, which defines the static friction coefficient μ_s .

Note that, strictly speaking, due to the finite loading stiffness K , sliding starts (depinning occurs) at a slightly lower force level. Indeed, when the peak is reached, necessarily, the instantaneous sliding velocity \dot{x} equals the driving one since, inertia being negligible, $K(V_0 - \dot{x}) = dF/dt = 0$ at this point. Close inspection of the F -trace indeed reveals, in the immediate vicinity of F_s , a small rounding off.

(iii) Beyond the static threshold, a rapid force drop is observed, and F reaches the steady state plateau value $\mu_d(V_0|t_0)W$.

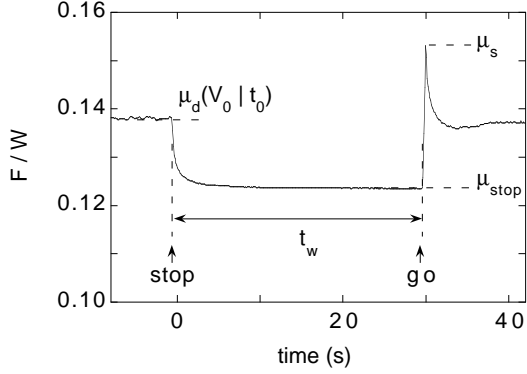


Fig. 3. Force trace corresponding to a stop-and-go experiment (see text), on a D5 track. $V_0 = 10 \mu\text{m}\cdot\text{s}^{-1}$, $t_0 = 10^4$ s. μ_{stop} corresponds to the jamming stress level; μ_s measures the static threshold.

Moreover, when varying the waiting time t_w over more than two decades, we observe (fig.4) that μ_s increases quasi-logarithmically with t_w : as time lapses, the interfacial pinning strength of the non moving system increases. Since this occurs at constant Σ_r , we must conclude that, when at rest, the adhesive joints experience *structural aging*.

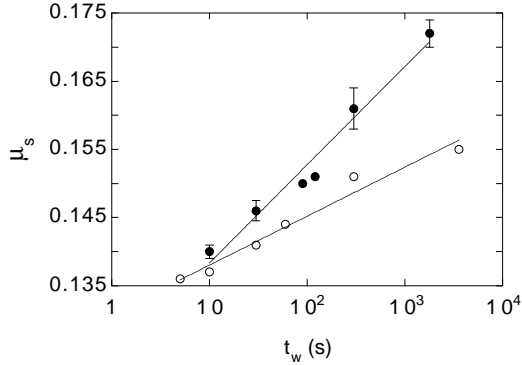


Fig. 4. Growth of the static friction coefficient with waiting time t_w , on a D5 track. (o): waiting under zero shear stress ($\mu_w = 0$). (bullet): waiting at the jamming level μ_{stop} .

A second important conclusion results from the presence of the post-peak stress drop in the transient characteristics. Indeed, this decrease of the interfacial strength indicates that, conversely, when sliding sets in, the “structural age” φ decreases from its initial value, reached after waiting t_w , to the smaller value $\varphi(V_0)$, reached when steady motion is established : *motion rejuvenates the adhesive joints*.

Structural aging is a robust phenomenon, which we have observed with all interface samples, involving either bare or silanized glass tracks.

The aging dynamics can be characterized by the value of the logarithmic slope $\beta_s = d\mu_s/d(\ln t_w)$. This is found to lie in the range $1.5 \times 10^{-3} - 5 \times 10^{-3}$. Although this

level of dispersion is well above experimental uncertainty, no correlation can be evidenced between β_s values and $\bar{\mu}$ levels.

3.3 Dependence of aging on shear stress level at rest

In the stop-and-go experiments described above, the system ages at rest under the finite shear force $F_{stop} = \mu_{stop}W$ at which its self decelerating creep becomes immeasurably slow. This “jamming force level” is found to lie at most 10% below the steady one $\mu_d W$ (see for example Figure 3).

The question then naturally arises of whether the shear stress level at rest affects the aging dynamics. For this purpose we have extended the standard stop-and-go protocol as follows. At time $t = 0$ the drive is reversed, so as to unload the system down to the desired “waiting” level $\mu_w W$, with $0 \leq \mu_w < \mu_{stop}$. After waiting t_w , we measure the height of the static peak $\mu_s(t_w|\mu_w)$.

Figure 4 shows the variations with waiting time of $\mu_s(t_w|\mu_{stop})$ and $\mu_s(t_w|0)$ for a D5 sample. The corresponding logarithmic slopes are respectively $\beta_s(\mu_{stop}) = 6.2 \times 10^{-3}$ and $\beta_s(0) = 3.7 \times 10^{-3}$. Clearly, the aging dynamics is markedly accelerated by the presence of the shear stress. This effect is observed with all samples.

It can be further qualified by measuring μ_s , for a given waiting time t_w , at various μ_w levels. The result of such a set of experiments, performed with four different silanized surfaces, is shown on Figure 5 for $t_w = 10$ s. In view of the spread of average friction levels, we have plotted, for the sake of comparison, the drop $\Delta\mu$ associated with the post peak stress drop, versus $(\mu_{stop} - \mu_w)$. It is seen that:

- To a good approximation, all data collapse on a single curve – indicating, again, a very weak correlation between aging dynamics and average friction level.
- The structural age reached at t_w decreases very rapidly as the waiting stress level decreases below the jamming one.

Note that some data correspond to $\Delta\mu = 0$, meaning that, in such cases, no static peak was observable after waiting $t_w = 10$ s. In these cases, upon loading, the end of the static regime is revealed by a break in the slope of the $F(t)$ trace. For these samples at such low μ_w , the static peak starts developing only for larger t_w (see Figure 6). Systematic investigations at $\mu_w = 0$ reveal that the corresponding “latency time” is strongly sample-dependent. We have observed values ranging from less than 10 s to more than 2000 s.

3.4 Velocity dependence of the steady sliding friction coefficient

We have also systematically measured the $\mu_d(V)$ characteristics of our geometrically old interfaces. A typical result is shown on Figure 7. $\mu_d(V)$ exhibits a minimum μ_{min} at $V = V_{min}$. For this D5 sample, $V_{min} \approx 1 \mu\text{m}/\text{s}$.

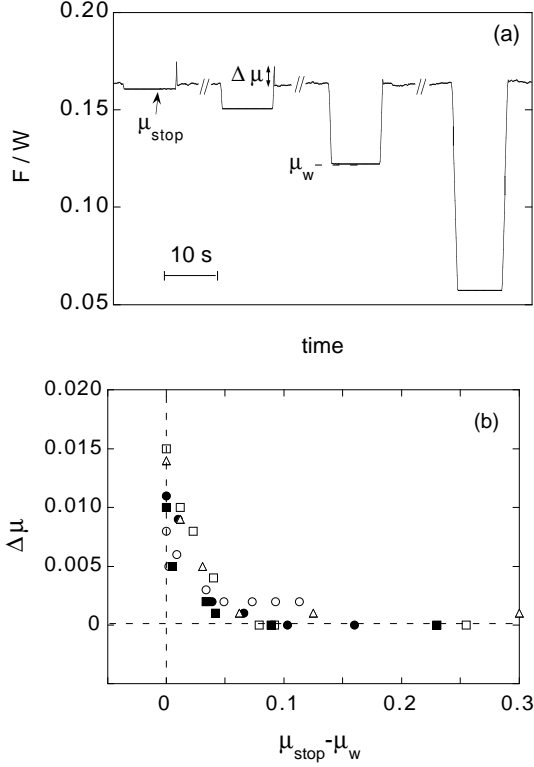


Fig. 5. (a) Force trace for a set of four stop-and-go runs on a D5 track at $V_0 = 10 \mu\text{m}\cdot\text{s}^{-1}$. Successive stops all last for $t_w = 10$ s, and are performed under decreasing μ_w levels. (b) Post static peak reduced stress drop $\Delta\mu$ versus $\mu_{\text{stop}} - \mu_w$, for three D1 (■, □, △) and two D5 (●, ○) tracks.

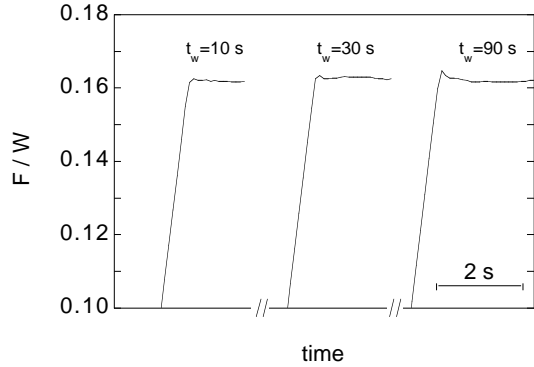


Fig. 6. Three force records for a D5 track, illustrating the behaviour when reloading after stops at $\mu_w = 0$ of increasing duration t_w . The static peak becomes visible after a latency time which, here, lies between 30 s and 90 s.

The velocity weakening observed for $V < V_{\text{min}}$ provides another evidence that the structural age φ decreases with V , i.e. that the system rejuvenates when sliding.

For $V > V_{\text{min}}$, μ_d exhibits clearly a logarithmic increase, reminiscent of that found for rough/rough (e.g. PMMA) interfaces. It has been shown that this effect can be attributed to thermally activated premature depinning of bistable centers with a volume on the order of a cubic

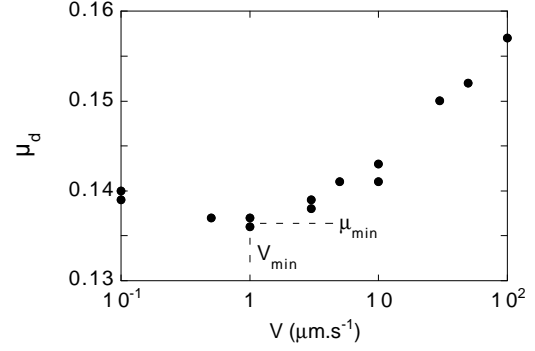


Fig. 7. Dynamic friction coefficient versus velocity V for a D5 sample.

nanometer. These centers would thus be the basic dissipative units within the sheared adhesive joint. It is this mechanism, which should also be at work here, which yields the V -dependence of the sliding stress given by equation (2). For PMMA at 300K, the dimensionless parameter appearing in this equation $\alpha \approx 5 \times 10^{-2}$.

For the sake of comparison, we have rescaled our $\mu_d(V)$ data by μ_{min} . The result, for five different (D1 and D5) samples is plotted on Figure 8, in which V has also been scaled by V_{min} . It is seen that, for $V/V_{\text{min}} > 1$, all data then collapse on a single curve. The common reduced logarithmic slope in the velocity-strengthening regime is $5 \times 10^{-2} \pm 6 \times 10^{-3}$, in full agreement with the previously evaluated α for PMMA/PMMA.

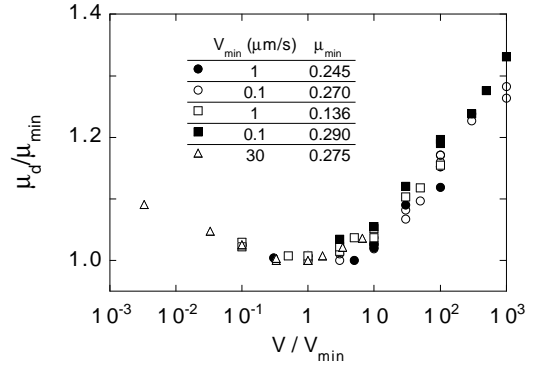


Fig. 8. Reduced (see text) dynamic friction coefficient μ_d/μ_{min} versus reduced velocity V/V_{min} for D1 (●, ○, ■, △) and D5 (□) tracks.

From this, one may also conclude that, already rather close above V_{min} , the sliding induced rejuvenation effect is quasi-saturated (which justifies a posteriori our choice of μ_{min} for the rescaling).

Note that, while the μ -levels for the various samples differ at most by a factor of 2, V_{min} values span more than two decades (from 0.1 to $30 \mu\text{m/s}$). This considerable scatter must certainly be related to the fact that aging/rejuvenation is associated with activated “jumps” above the barriers of a glass-like energy landscape. Hence,

roughly speaking, an exponential sensitivity to variations of this landscape.

Velocity-weakening is well known to promote stick-slip instabilities. Indeed, we did observe stick-slip oscillations for silanized samples, but only for a few of the D1 ones, and in the lower part of their V -weakening regime. Let us recall that, as long as the rejuvenation mechanism responsible for weakening is non-instantaneous, a negative $d\mu_d/dV$ does not necessarily entail stick-slip, the presence of which is governed by the detailed dynamics of the age variable and by the external control parameters, e.g. the external loading stiffness.

It is worth mentioning that, with bare glass tracks, we always observe stick-slip, up to a strongly sample-dependent velocity threshold, ranging from $\sim 10\mu\text{m/s}$ to $> 100\mu\text{m/s}$. That is, as a rule of thumb, the higher the average friction level, the stronger the trend towards destabilization of steady sliding. However, the poor reproducibility of systems involving bare glass does not permit to make this statement more quantitative.

3.5 Long lasting transients

While, for D5 tracks, the transient behavior only consists of the above described static peaks, for D1 systems a more complicated dynamics emerges. Indeed (see Figure 9), in most cases, the force traces also exhibit long lasting post-peak bump shaped transients. Comparison of data for various driving velocities spanning about a decade enable us to assert that this slow transient is not governed by a characteristic time but, rather, by a slid length lying in the $100 - 300 \mu\text{m}$ range. This must be contrasted with the distance slid during an initial stress drop, which never exceeds $1 \mu\text{m}$, indicating that the associated mechanisms are of a different nature.

Moreover, the bump amplitude is found to increase markedly as the waiting stress level is decreased (Figure 9).

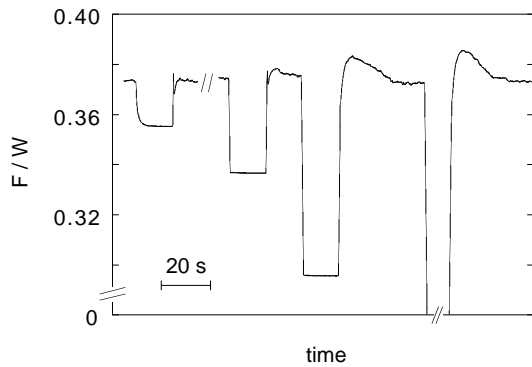


Fig. 9. Long lasting bump shaped transients, after four stops of duration $t_w = 20$ s, illustrating the increase of transient bump amplitude with decreasing μ_w level.

These elements lead us to associate long lasting transients with anelastic evolution of the slider PMMA mol-

ecules forming the joints: when the stress level is stepped down, as occurs during a stop, they are likely to experience strain recovery. Upon reloading, this process is reversed, and the corresponding work must be provided by the external force.

That this mechanism is attributable to conformational evolution of the surface region of the slider is proved by the fact that these long transients are most pronounced when using freshly lapped PMMA surfaces. Bump heights then decrease gradually with cumulated slid distance, on scales of the order of tens of centimeters. Large bumps reappear after relapping. This suggests that repeated stress cycling leads to irreversible alignment of the polymer molecules – an effect documented already long ago by Tabor *et al* [19], in particular with PTFE, for which it is most pronounced.

4 Discussion

The set of experimental results reported in Section 3 leads us to assert that the nanometer-thick adhesive joints in which frictional sliding localizes can be considered in all respects as a confined 2D soft glass medium, or, equivalently, threshold fluid. Namely :

- (i) Below a static threshold, it responds elastically: it is pinned in a disordered solid state induced by confinement under the normal stress.
- (ii) This static threshold increases logarithmically with the waiting time : when at rest, the joint ages.
- (iii) When sliding starts, the stress drops until reaching its (lower) stationary level : motion rejuvenates the joint.
- (iv) This rejuvenation corresponds to the existence of a velocity-weakening regime for dynamic friction. As V increases, rejuvenation saturates and friction becomes velocity-strengthening.

Moreover, we find that the (logarithmic) aging rate increases markedly with the shear stress applied to the system at rest. This influence on aging of stress during waiting is akin to the recent results obtained by Viasnoff *et al* [20] with a colloidal glass. They have shown that applying to this system, aging under stress-free conditions, an oscillating shear stress of finite duration does result in a strong perturbation of the aging process.

In our stop-and-go experiments, the whole aging process takes place under constant shear below the static threshold. This situation is reached after performing a “mechanical quench”, during which sliding decelerates and stops at the prescribed level. Note that the duration Δt of the quench depends on the final stress level : for the largest one, corresponding to the jamming level μ_{stop} , it is determined by the sliding dynamics itself, and is typically a few seconds. When we unload below μ_{stop} , Δt is controlled by the unloading time – at most 1 second. For some samples at $\mu_w = 0$, no static peak is observed for a finite latency period. This indicates that, in these experiments (i) unloading has been fast enough for the joints to be quenched at the initial age $\varphi(V_0)$ they had when sliding; (ii) the subsequent aging dynamics is slow enough that the peak growth is too small to be measured up to the latency time.

The aging rate increase with waiting stress level is most likely ascribable to the associated biasing of the energy landscape and to the corresponding decrease of “trap depths” [9,10]. This effect might be responsible in part for the observation by Berthoud *et al* [3] that the logarithmic growth rate of the static peak height of a {rough/rough} PMMA interface is larger under jamming than under stress-free conditions. It would be of interest that analogous studies be performed with 3D threshold fluids such as colloidal glasses.

While the above described phenomenology of friction exhibits all the main qualitative features of soft glass rheology, when inspected more closely, our results lead to two further questions.

(i) The logarithmic velocity dependence of the dynamic friction coefficient μ_d in the strengthening regime is fully compatible with a description in terms of premature depinning events induced by the thermal noise, as discussed in references [2,7]. Existing theories of sheared glasses [9,10,11] and of plasticity of amorphous media [21,22] lead to the idea that, while thermal noise should be relevant at low shear rates, beyond some crossover, the dynamical noise associated with the depinning events themselves should take over. No prediction is available for the moment about the position of this crossover.

In our experiments, the V -strengthening regime corresponds to shearing rates $\dot{\gamma} = V/h \simeq 10^3\text{--}10^5$. This seems to indicate that, for frictional joints, the $\dot{\gamma}$ crossover value would be at least that huge. Whether this rather surprising result is of some degree of generality, or is due to possible screening of elastic interactions related with the confinement of our 2D medium remains an open question.

(ii) Average friction levels are highly sensitive to the chemical differences between surfaces obtained under nominally identical silanization conditions. This is most probably related with the fact that defects in the silane coverage, however small their scale, leave non passivated high energy, strong pinning sites on the glass surface. These lead to strong corrugations of the confining potential, hence of the glass-like energy landscape. The impossibility to correlate our β_s and $\bar{\mu}$ data leads us to suspect that, while $\bar{\mu}$ measures an average pinning strength, β_s might be sensitive to much finer details of the landscape. Numerical modelling would probably be very helpful to shed light on this question.

We are indebted to J.M. Berquier and P. Silberzan for advice about glass silanization. We thank L. Leger, L. Cugliandolo and J. Kurchan for illuminating discussions.

References

1. F.P. Bowden and D. Tabor, *The Friction and Lubrication of Solids I* (Clarendon Press, Oxford, 1950).
2. T. Baumberger, P. Berthoud and C. Caroli, Phys. Rev. B **60**, 3928 (1999).
3. P. Berthoud, T. Baumberger, C. G’Sell and J.-M. Hiver, Phys. Rev. B **59**, 14313 (1999).
4. M. Nakatani, J. Geophys. Res. **106**, 13347 (2001).

5. C.H. Scholz, *The Mechanics of Earthquakes and Faultings* (Cambridge University Press, Cambridge, 1990).
6. F. Heslot, T. Baumberger, B. Perrin, B. Caroli and C. Caroli, Phys. Rev. E **49**, 4973 (1994).
7. B.N.J. Persson, *Sliding Friction*, Nanoscience and Technology Series (Springer, Heidelberg, 1998).
8. G. He and M.O. Robbins, Phys. Rev. E **64**, 035413 (2001).
9. S.M. Fielding, P. Sollich and M.E. Cates, J. Rheol. **44**, 323 (2000).
10. P. Sollich, Phys. Rev. E **58**, 738 (1998).
11. L. Berthier, J.-L. Barrat and J. Kurchan, Phys. Rev. E **61**, 5464 (2000), and references therein.
12. C. Derec, A. Ajdari and F. Lequeux, Eur. Phys. J. E **4**, 355 (2001).
13. B. Abou, D. Bonn and J. Meunier, Phys. Rev. E **64**, 021510 (2001).
14. M. Cloitre, R. Borrega and L. Leibler, Phys. Rev. Lett. **85**, 4819 (2000).
15. C. Derec, PhD thesis, Université Paris VII (2001).
16. J. Dieterich and B. Kilgore, Pure Appl. Geophys. **143**, 283 (1994).
17. B. Kilgore (private communication).
18. J.M. Berquier (private communication).
19. C.M. Pooley and D. Tabor, Proc. R. Soc. Lond. A **329**, 251 (1972).
20. V. Viasnoff and F. Lequeux (to be published).
21. A.S. Argon, V.V. Bulatov, P.H. Mott and U.W. Suter, J. Rheol. **39**, 377 (1995).
22. M.L. Falk and J.S. Langer, Phys. Rev. E **57**, 7192 (1998).